

Hg(II) adsorption by alginate-guar gum templated titania spheres: Kinetic and isotherm studies

Vandana Singh*, Preeti, Angela Singh, Devendra Singh, Jadveer Singh, Arvind K Pandey, Tulika Malviya

Department of Chemistry, University of Allahabad, Uttar Pradesh 211002, India

*Corresponding author. Tel: (+91) 9415310942; (+91) 8127598952; E-mail: singhvandanasingh@rediffmail.com

Received: 25 February 2015, Revised: 30 April 2015 and Accepted: 06 June 2015

ABSTRACT

In present communication we report on the kinetic and isotherm studies on Hg(II) removal using our recently reported material, the millimeter sized hollow titania spheres (TSP). The mesoporous spheres with high surface area ($11.75 \text{ m}^2/\text{g}$) and bimodal pore size distribution were fabricated by a facile sol-gel approach using alginate-guar gum hybrid beads as the structure directing agent. In order to investigate the utility of TSP for Hg(II) adsorption, the batch adsorption experiments were conducted at various pH values (2–7), initial Hg(II) concentrations (50–300 mg/L), and TSP doses (20–100 mg) at 150 rpm, and 30 °C temperature. The spheres exhibited good capacity to adsorb Hg(II) in wide pH range (pH 3 to pH 7). It was possible to remove >95 % Hg(II) from 100 mg/L synthetic Hg(II) solution at pH 5, and 50 mg TSP dose in 10 h. The adsorption equilibrium data were better fitted to Langmuir model at low temperatures while Freundlich model become favored as the temperature was increased to 40 °C. Langmuir adsorption isotherm study indicated that the monolayer adsorption capacity of TSP was 62.5 mg/g 62.5 mg/g 78.7 mg/g and 100 mg/g at 10, 20, 30, and 40 °C respectively, which suggested good Hg(II) adsorption capacity of TSP. The calculated R_L values evidenced the feasibility of the adsorption. Adsorption kinetic data well accorded with pseudo-second order kinetic model with the rate constant k , equal to $2.5 \times 10^{-4} \text{ g/mg}\cdot\text{min}$ $1.99 \times 10^{-4} \text{ g/mg}\cdot\text{min}$ and $0.28 \times 10^{-4} \text{ g/mg}\cdot\text{min}$ at 100, 150 and 200 mg/mL initial Hg (II) concentrations, indicating chemisorption taking place in the rate determining step. At high initial Hg(II) concentration (200 mg/mL), the adsorption was exclusively controlled by intraparticle diffusion. The study revealed the suitability of TSP for the mercury removal from waste water. Copyright © 2015 VBRI press.

Keywords: Titania spheres; guar-alginate hybrid beads; Hg(II); adsorption.

Introduction

The strict regulations for water pollution prevention have attracted the development of newer methods/materials for improving water quality [1-4]. Among the heavy metal pollutants, mercury is one of the most hazardous metals as it bioaccumulates within living systems [5]. High solubility of Hg(II) in the hydro-system allows the entry of Hg(II) in the food chain to cause serious health hazards in the living systems.

In the dissolved phase mercury can exist in the form elemental mercury (Hg^0), ionic [$\text{Hg}(\text{II})$], and organic mercury (MeHg and Me_2Hg) [6]. Mercury contaminated water has many detrimental effects on aquatic environment and on the human health. In human, mercury poisoning is known to cause rheumatoid arthritis, minamata disease, diseases of the kidneys, circulatory system, nervous system, damaging of the fetal brain, paralysis and chromosome breakage etc. [7, 8]. Thus mercury toxicity has become a major apprehension at regional, national, and international

platforms. Many processes such as adsorption, coagulation, ion exchange, membrane technology, and chemical precipitation are known for Hg(II) removal from the aquatic environment [9]. Adsorption is popular technique in water treatment because of its low cost, simplicity of design, high efficiency and easy operation [10].

TiO_2 based materials are attractive due to their unique electronic and optical properties. They find application in photocatalytic degradation of organic pollutants, photolysis of water, solar cells, biomaterials, environmental catalysts, photovoltaics and energy storage [11-13]. Highly porous inorganic TiO_2 beads are endowed with excellent chemical and thermal stability, abundance, low cost, low density and low toxicity [14, 15]. Owing to uniqueness of their characteristics, they have been used as adsorbents for the removal of NO and acetone vapors [16], for fluoride removal [17], and for the removal of heavy metal ions [18].

Adsorbents consisting of hollow inorganic spheres can be easily recycled because of their easy separation from the reactor tanks [19-21] which is otherwise difficult for the

adsorbents of fine particle morphology. The column clogging problems in column studies can also be minimized by the use of hollow inorganic spheres as adsorbent. For enhancing the properties of such materials, the process parameters of their sol-gel synthesis and calcination temperature can be varied besides controlling the templating bead properties such as bead diameter, morphology, monodispersity, surface properties and porosity [13].

We recently reported [22] the sol gel synthesis and characterization of sodium alginate-guar gum hybrid bead templated millimeter sized titania spheres (TSP) where the mixed biopolymeric beads consisting of alginate and guar gum were used as templating scaffolds for titanium(IV) isopropoxide polymerization. The hybrid beads so obtained were calcined in air to obtain hollow spheres (TSP) which were shown to have good ability to capture Hg(II) ions from aqueous solution in a preliminary investigation. To understand the adsorption behavior of TSP, in the present study we have under taken a detailed kinetic and isotherm study on Hg(II) adsorption at TSP for the first time. The influence of pH, adsorbent dose, initial Hg (II) concentration, and temperature on Hg(II) adsorption by TSP was also studied to find out possibility of its exploitation for mercury removal in waste water remediation.

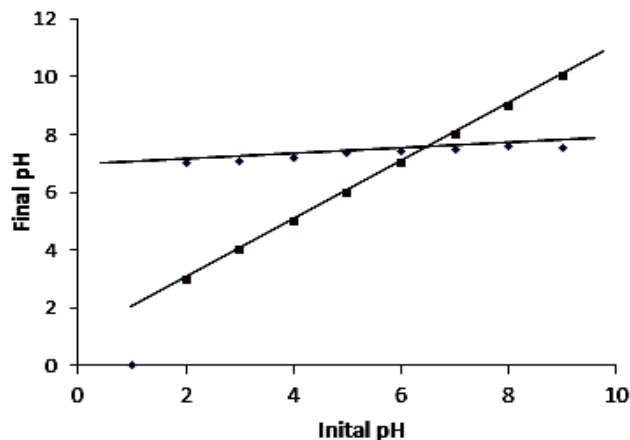


Fig. 1. Determination of pH_{ZPC} of TSP using pH drift method.

Experimental

Materials

Titanium (IV) isopropoxide (97%) and 2-propanol (99 %) were obtained from Aldrich and Merck, India respectively. Absolute ethanol (99.9%) A.R was from Changshu Yangyuan Chemical, China. Sodium alginate (Food grade; Assay 91-106%) and Rhodamine 6G were purchased from Loba Chemie Pvt Ltd., Mumbai, India. Guar gum calcium chloride (fused) (Assay 98 %), mercury (II) chloride (G.R) (99.5 %), potassium iodide (G.R) Assay 99.8 %, potassium hydrogen phthalate (G.R) (99.9-100 %), were all purchased from Merck, India. Sodium thiosulphate (A.R) and gelatin (bacteriological) were from central drug house (P) Ltd., India and Qualigens fine chemicals, Thermolectron LLS India Pvt. Ltd., Mumbai respectively. Double distilled water was used in all the procedures. The

pH values were adjusted by the addition of 5 M HCl (G.R, Merck, India, 35%); or 1 M NaOH (Merck, India).

Methods

pH measurements were done using EUTECH pH meter (model 510). Temperature treatment was done in microprocessor controlled electric muffle furnace, Metrex Scientific Instruments (P) Ltd., New Delhi, India. Orbital shaker incubator, Metrex Scientific Instruments (P) Ltd., New Delhi was used. All experiments were done in three sets and readings reported are the average of three reading.

Synthesis and characterization of TSP

The adsorbent (TSP) was synthesized and extensively characterized as described elsewhere [22]. In brief, a solution of guar gum (0.25 g) and alginate (0.25 g) in H_2O (25 mL) was dropped through 2 mm diameter nozzle into aqueous Ca^{2+} bath (100 mL of 0.2 M $CaCl_2$ solution) to obtain mixed polysaccharide beads which were cured in 0.2 M calcium chloride solution for 2.5 h and thereafter washed well with water to remove the adhered Ca^{2+} . The swollen beads were dehydrated by equilibration using solvent exchange from water (75 mL) to ethanol and finally in isopropanol for 3 h in each and then were soaked in the 7:3 v/v mixture of titanium isopropoxide and isopropanol for 16 h at room temperature and were finally hydrolyzed with water/isopropanol solution 1:1(v/v) (5 mL each). The hybrid titania beads so obtained were washed well with water and were dried in an oven for 8 h at 35-40° C. The dried beads were calcined at 450°C for 2 h under air flow to obtain the adsorbent (TSP).

Determination of pH_{ZPC}

pH_{ZPC} of TSP was determined by pH drift method for which a solution of 0.005M $CaCl_2$ was boiled to remove the dissolved CO_2 and then cooled down to room temperature. The pH of the solution was adjusted to a value between 2 and 10 using 2.5 M HCl or 5 M NaOH. The TSP (50 mg) was added into 20 mL of the pH adjusted solution in a capped vial and equilibrated for 48 h. The final pH was measured and plotted against the initial pH. The pH at which the curve crosses the $pH_{initial} = pH_{final}$ line was taken as pH_{ZPC} [23] (Fig. 1).

Hg(II) removal

Hg(II) adsorption was monitored using batch adsorption study. Hg(II) stock solution (1000 mg/L) was prepared by dissolving an appropriate amount of $HgCl_2$ in deionized double-distilled water. Batch adsorption experiments were carried out using TSP as adsorbent on a temperature-controlled incubator shaker set at 150 rpm (the rpm variation showed optimum result at 150 rpm; rpm optimization is not shown) and maintained at 30 °C. The adsorbent (50 mg) was left in an incubator shaker with Hg(II) solution (20 mL of 100 mg/L) for a desired time period, and then filtered through a Whatman 0.45 mm filter paper. After suitable dilution, the remaining Hg(II) was estimated spectrophotometrically at $\lambda 575$ nm using Rhodamine 6G dye in the presence of iodine buffer [24]. The amount of metal ions adsorbed per gram of the TSP

was calculated by the difference between the initial and final Hg(II) concentrations using the Eq. (1)

$$q_e(\text{mg/g}) = \frac{C_0 - C_e (\text{mg/L}) \times V(\text{L})}{W(\text{g})} \quad (1)$$

where q_e is the amount of the metal adsorbed (mg/g) onto the adsorbent, C_0 is the initial concentration of the metal (mg/L), C_e the equilibrium concentration of the metal in solution (in mg/L), V the volume of the solution used (L), and W the weight of the TSP used as adsorbent. All the adsorption experiments were performed in triplicates and the results presented are the average of three readings.

For optimization study, pH variation was done in the pH range of 4–10 at 100 mg/L initial Hg(II) concentration, 50 mg TSP dose, 10 h contact time, and 150 rpm at 30 °C, while adsorbent (TSP) doses of 20–100 mg were contacted for 10 h with 20 mL of 100 mg/L Hg(II) solution at 30 °C and 150 rpm. Adsorption of Hg(II) at various initial concentrations, ranging from 25 to 350 mg/L was studied at pH 5, 50 mg TSP dose, 10 h contact time, and 150 rpm at temperatures ranging from 10 to 40 °C. The kinetic study was performed at 150, 200 and 250 mg/L initial Hg(II) concentrations, using 50 mg of TSP dose, pH 5, rpm 150 and temperature 30 °C.

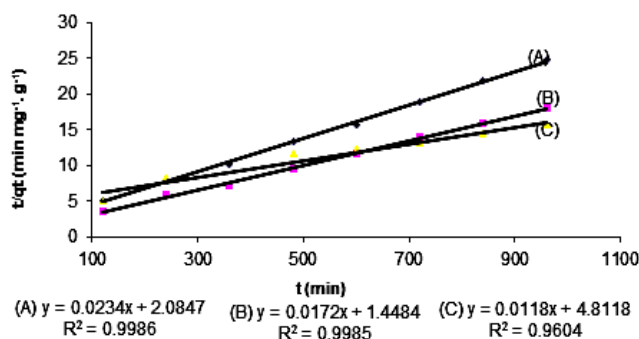


Fig. 2. Pseudo second order kinetic models for adsorption at (A) 150, (B) 200 and (C) 250 mg/L Hg(II) concentrations, at 50 mg of adsorbent dose, 150 rpm, pH 5 and temperature 30 °C.

Results and discussion

Mn TSP and mercury loaded TSP were characterized by IR, XRD, SEM and TEM studies as described elsewhere [22]. The hybrid Titania spheres are nanoporous material with interconnected bimodal pores. The material has a surface area of 11 m²/g [22] with pore distribution ranging from 1.2 to 9 width. The size of the void between the ridges of the spheres is ~50 μm. As characterized in our previous study [22], TSP spheres consist of aggregated TiO₂ nanoparticles of 10–12 nm size. pH drifts experiments indicated that TSP has pH_{zpc} of 6.2 and its surface has zero surface charge at this pH. The material characteristics and our previous preliminary investigations [22] revealed that TSP can be exploited as an effective Hg(II) adsorbent. To understand its adsorption behavior and to work out the feasibility of its use in Hg(II) removal from wastewater, in the present study we undertake a detailed study on the

adsorption isotherms and kinetics at our recently synthesized and characterized material “TSP” [22].

Sorption kinetics

The kinetic study revealed that the rate of the adsorption was initially fast which attained equilibrium in 10 h [24, 25]. In first 8 h about 89% of the initial Hg(II) was adsorbed and then the adsorption slowly tapered off. The initial high adsorption rate is due to the availability of free adsorption site at the beginning of the adsorption, which declined slowly with the passage of the time. The kinetic data were modeled by the first order Lagergren equation and pseudo-second-order equations. The linear expressions for the above models are given in Eq. (2) to Eq. (3) respectively.

$$\log(q_e - q_t) = \log q_e - \frac{k_1}{2.303} t \quad \text{--- (2)}$$

$$\frac{t}{q_t} = \frac{1}{k_2 q_e^2} + \frac{t}{q_e} \quad \text{--- (3)}$$

Where, k_1 and k_2 are constants for pseudo first order and pseudo second order models respectively. The kinetic data (Table 1) of the present study accorded well with pseudo second order kinetic equation indicating chemisorption taking place in the rate determining step involving various forces through sharing or exchange of electrons between sorbent and sorbate. Linear plot of t/q_t vs t (Fig. 2) had a correlation coefficient (R^2) of 0.9986 which indicated this model is best suited for the adsorption. At 150 mg/L initial Hg(II) concentration, the pseudo second order rate constant was calculated to be 2.5×10^{-4} . The parameters calculated using various kinetic models at various initial Hg(II) concentrations are presented in the Table 1, from which it is evident that the sorption data satisfy the pseudo second order kinetic model. The theoretically predicted q values increased with increasing initial Hg(II) concentration which is explainable as the amount of Hg(II) adsorbed should increase with increasing initial Hg(II) concentration [26] being adsorption a surface phenomenon.

Table 1. Constants derived for various kinetic models for Hg(II) sorption at TSP.

[Hg(II)] Mg L ⁻¹	Pseudo second order			Lagergren's			Weber moris		
	q_e mg g ⁻¹	k_2 g/mg /min	R^2	q_e mg/g	k_1 /min	R^2	k_d mg/g min ^{0.5}	R^2	
100	43.4	2.5×10^{-4}	0.9986	40.2	4.606×10^{-3}	0.964	1.48	0.9997	
150	58.8	1.99×10^{-4}	0.9985	29.3	4.606×10^{-3}	0.998	2.01	0.9889	
200	84.7	2.8×10^{-5}	0.9604	84.5	2.303×10^{-3}	0.896	1.96	0.974	

Since neither pseudo first order nor pseudo second order model can identify the diffusion mechanism, it was necessary to model the kinetic data by intraparticle diffusion model using Eq. (4). The rate cannot be decided only by the mass transfer from the bulk liquid to particle's external surface as the particles were rapidly agitated during the sorption period. It may be assumed that the rate determining step may be film or intraparticle diffusion.

Weber and Morris intraparticle diffusion model is expressed as eq-4

$$q_t = k_{id} \times t^{0.5} + C \quad \text{--- (4)}$$

Where q_t (mg/g) is amount of mercury adsorbed at time t , C is (mg/g) intercept and k_{id} (mg/g min^{0.5}) is the intraparticle diffusion rate constant. Some degree of boundary layer control was indicated at 100 and 150 mg/L initial Hg(II) concentration as the plots of q_t vs $t^{0.5}$ did not pass through origin and plot has intercept 7.2 mg/g and 5.1 mg/g respectively, indicating that intraparticle diffusion is not only the rate determining step but other kinetic mechanism may be controlling the rate of sorption and all of them may be operating simultaneously. High intercept at these Hg(II) concentrations is the indicative of the abundance of the solute in the boundary layer. According to McKay and Allen [27], three linear sections on the plot q_t vs $t^{0.5}$ can be identified. The first portion represents external surface adsorption or an instantaneous adsorption stage while the second portion is a gradual adsorption stage, where the intra-particle diffusion is the controlling factor and final equilibrium stage where the intra-particle diffusion starts to decelerate due to extremely low solute concentrations in the solution. At 100 and 150 mg/L initial Hg(II) concentrations first two sections are visible while the third section is not visible in the present study.

A linear plot passing through origin was obtained for 200 mg/L initial Hg(II) concentration, indicating intraparticle diffusion is the only rate determining step at this high initial Hg(II) concentration (**Fig. 3**).

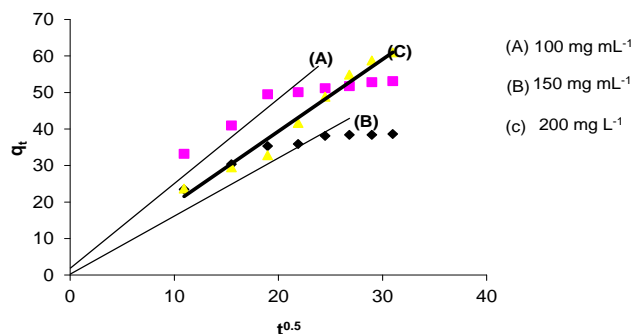


Fig. 3. Weber and Morris intraparticle diffusion model for the adsorption kinetic data at 100, 150 and 200 mg/L initial Hg(II) concentrations, pH 5, 30 °C, rpm 150, 50 mg TSP dose, 20 mL contact volume.

Optimization of adsorption

Adsorption pH

The pH is a controlling factor while assessing the sorption capacity of an adsorbent for determining the adsorption between the adsorbent and aqueous interface. The uptake of Hg(II), onto TSP for 100 mg/L initial Hg(II) concentration and 50 mg TSP dose has been examined in the pH range of pH 2–10. **Fig. 4(a)** shows the uptake of metal ions by TSP as a function of pH where a sharp increase in the adsorption is visible on increasing the pH from pH 2 to pH 3, thereafter it did not change much up to pH 6 (~95% uptake). The adsorption decreased to 93% when pH was increased to pH 7. Thus it is evident that the adsorbent could perform very well in wide pH range (pH 3 to pH 7).

The availability of surface hydroxyl groups at TiO₂ is dependent on the solution pH. TSP surface charge will be zero at pH 6.2, it will be negative at pH >pH_{zpc} and positive at pH <6.2. At measurement pH, pH 5, the TSP has Ti-OH and/or Ti-OH₂⁺ however surface hydroxyl groups of TiO₂ will be dissociated to form TiO⁻ at pH > 6.2 [7]. Many mercury species such as (HgCl₂, HgCl⁺, HgClOH, and Hg(OH)₂) are present in the pH range 3.0 -7.0. Thus electrostatic interaction does not seem to be reason for the adsorption in the present study; rather it appears to be surface phenomenon where mercury species is physically adsorbed at TiO₂ nanoparticle surface of the spheres.

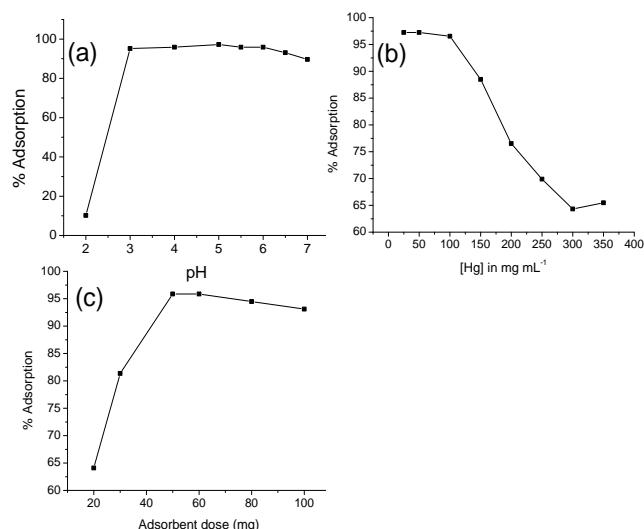


Fig. 4. Effect of (a) pH (b) initial Hg(II) concentration (c) adsorbent dose on Hg(II) adsorption by TSP. The adsorption conditions: initial Hg(II) concentration 100 mg/L, TSP dose 50 mg, contact time 10 h, rpm 150, temperature 30 °C.

Initial Hg(II) concentration

Adsorption of Hg(II) at various initial Hg(II) concentrations ranging from 25 to 350 mg/L is demonstrated at optimum pH (pH5), 10 h contact time, 150 rpm and temperature 30 °C (**Fig. 4(b)**). It was found that with the increase in the initial Hg(II) concentration from 50 to 350 mg/L the removal of Hg(II) declined from 97 % to 65%. This is explainable as at higher initial Hg(II) concentrations more Hg²⁺ ions are available for the fixed available adsorbing sites at the sorbent.

Adsorbent dose

In order to investigate the effect of adsorbent (TSP) dose on Hg(II) adsorption, various doses of adsorbent (20-100 mg) were contacted with 20 mL of 100 mg/L Hg(II) solution for 10 h at 30 °C, and 150 rpm. It is apparent that the % adsorption increased with the increase in the adsorbent dose. **Fig. 4(c)** shows that adsorption capacity increased from 64% to 93 % with the increase in adsorbent dose from 10 to 50 mg. This can be attributed to the availability of additional binding sites at higher doses. It was observed that the amount of Hg (II) adsorbed on TSP increased with increase in the adsorbent dose up to 50 mg and further increase in dose did not affect the removal much, indicating exhaustion of Hg(II) for further adsorption.

Adsorption isotherm study

Equilibrium relationships between adsorbent and adsorbate are important in designing a sorption system. The adsorption isotherms describe the maximum capacity of adsorption of an adsorbent. In the present study two adsorption isotherm models, Langmuir and Freundlich [28] have been considered to describe the adsorption equilibrium. Langmuir isotherm may be represented in the linear form by the eq-5.

$$\frac{C_e}{q_e} = \frac{1}{Q_o b} + \frac{C_e}{Q_o} \quad \text{---- (5)}$$

Where, C_e is equilibrium concentration (mg/L), q_e the amount of mercury ions sorbed (mg/g) at equilibrium, Q_o and b are Langmuir constants related to adsorption capacity (mg/g) and energy of adsorption (mg/L) respectively. The constants values were calculated from the slope and intercept of the linear plot. The essential features of Langmuir adsorption isotherm can be explained in terms of a dimensionless constant 'separation factor' or equilibrium parameter R_L which can be calculated using the eq. 6.

$$R_L = \frac{1}{(1 + bC_e)} \quad \text{---- (6)}$$

Where, C_o is the initial concentration of metal ions. The value of R_L reveals that the Langmuir isotherm to be either unfavorable ($R_L > 1$), linear ($R_L < 1$), favorable ($0 < R_L < 1$) or irreversible ($R_L = 0$). The correlation coefficient value R^2 nearer to one suggests that the isotherm equation better fits the experimental data [14].

The Freundlich isotherm model is an empirical model that describes the multilayer sorption and intensity of the sorption onto adsorbent.

The linear form of Freundlich isotherm model is expressed by the following equation:

$$\log q_e = \text{Log } K_F + 1/n \log C_e \quad \text{---- (6)}$$

Where Q_e = the amount adsorbed (mg/g) at equilibrium time, C_e = concentration of the Hg(II) at equilibrium (g/L), Freundlich constants K_F shows adsorption capacity of the adsorbent and "n" shows the adsorption intensity.

The adsorption equilibrium data better fitted to Langmuir isotherm in the temperature range of 10 to 30 °C, however, as the temperature was increased to 40 °C, the equilibrium data could be successfully fitted to both the models, indicating the adsorption phenomenon at high temperature was complex which involved more than one mechanism. The adsorption isotherms are shown in Fig. 5. The maximum monolayer adsorption capacity (Q_o) and b for TSP were calculated to be 78.7 mg/g and 0.1467 L/mg respectively (at 30 °C). At this temperature R_L value was calculated to be 0.0638, which is < 1 , hence the adsorption is favorable nature. A favorable adsorption was indicated by K_f (adsorption capacity (mg/g)) and n (an empirical parameter related to the intensity of adsorption) values which were calculated to be 25.06 and 3.60 respectively

from the Freundlich isotherm derived at 30 °C. The linear form of Freundlich isotherm is shown in Fig. 5. The value of n is greater than one is an indication that significant adsorption takes place. The high value of K_F is indicative of good adsorption intensity [14].

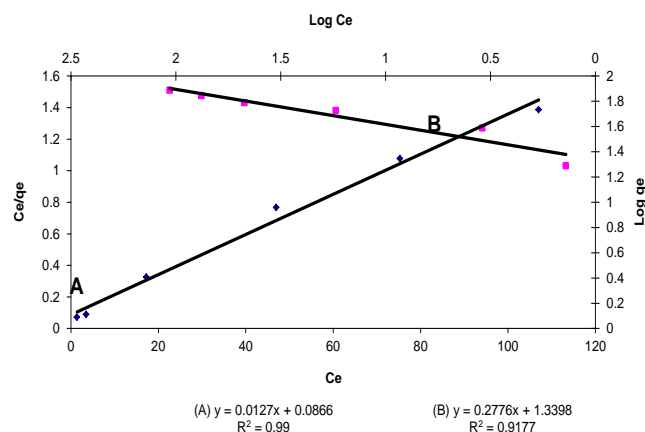


Fig. 5. Langmuir and Freundlich adsorption isotherms at 100 mg/mL initial Hg(II) concentration, pH 5, 30 °C, rpm 150, 50 mg adsorbent dose, 20 mL contact volume.

Table 2 Summarizes Langmuir and Freundlich constants calculated from isotherms derived at various temperatures.

Temperature (°C)	Langmuir Constants			Freundlich Constants		
	Q_o (mgg ⁻¹)	b (L mg ⁻¹)	R^2	K_f (mgg ⁻¹)	n	R^2
10	62.6	1.3333	0.971	31.41	5.68	0.531
20	62.5	1.2307	0.971	38.64	12.5	0.071
30	78.7	0.1467	0.99	25.06	3.60	0.917
40	100	0.1111	0.948	22.49	3.07	0.984

Conclusion

TSP showed pretty good (62-100 mg/g) Q_{max} (equilibrium mercury adsorption capacity) in a temperature range of 10-40 °C and the adsorption equilibrium could be established within 10 h. The adsorbent is usable in wide pH range (pH3 to pH 7). At lower temperatures (10-20°C) the adsorption equilibrium data could be explained by Langmuir model, while $> 20^\circ\text{C}$, the data could be modeled well by both the isotherms, indicating that the adsorption was complex at high temperatures and involved more than one mechanism. The adsorption equilibrium data confirmed to the pseudo second order kinetic model which indicated that chemisorption is involved in the rate determining step. It was indicated that at lower initial Hg(II) concentrations, intraparticle diffusion is not only the rate determining step while at 200 mg/L initial Hg(II) concentration, rate was exclusively controlled by intraparticle diffusion. TSP derived from guar-alginate hybrid beads and titanium (IV) isopropoxide proved to be an efficient adsorbent for Hg(II) ions from synthetic Hg(II) solutions and the adsorbent can be useful for waste water remediation.

Acknowledgements

Preeti acknowledge Council of Scientific and Industrial Research, India for the financial support to carry out the present work.

Reference

- Zhang, W.-x. *J. Nanopart. Res.*, **2003**, 5, 323.
DOI: [10.1023/A:1025520116015](https://doi.org/10.1023/A:1025520116015)

2. Horikoshi, S.; Hidaka, H. *Environ. Sci. Technol.*, **2002**, *36*, 1357.
DOI: [10.1021/es010941r](https://doi.org/10.1021/es010941r)
3. Kumar, R.; Abraham, T.N.; Jain, S.K. *Adv. Mater. Lett.*, **2012**, *3*, 507.
DOI: [10.5185/amlett.2012.icnano.138](https://doi.org/10.5185/amlett.2012.icnano.138)
4. Srivastava, S. *Adv. Mater. Lett.* **2013**, *4*, 2.
DOI: [10.5185/amlett.2013.icnano.11](https://doi.org/10.5185/amlett.2013.icnano.11)
5. Morel, F.M.M.; Kraepiel, A.M.L.; Amyot, T. M. *Annu. Rev. Ecol. Syst.*, **1998**, *29*, 54.
DOI: [0066-4162/98/1120-0543\\$08.00](https://doi.org/10.1146/annurev.ecolsys.29.1.54)
6. Boszke, L.; Głosińska, G.; Siepak, J. *Pol. J. Envir. Stud.*, **2002**, *11*, 285.
DOI: [10.2478/v10009-007-0020-7](https://doi.org/10.2478/v10009-007-0020-7)
7. Bernhoft, R.A. *J. Environ. Public Health* **2012**, *2012*, 460.
DOI: [10.1155/2012/460508](https://doi.org/10.1155/2012/460508)
8. D'Itri, F.M. *Environ. Monit. Assess.* **1991**, *19*, 165.
DOI: [10.1007/BF00401309](https://doi.org/10.1007/BF00401309)
9. Fu, F.; Wang, Q. *J. Environ. Managem.* **2011**, *92*, 407.
DOI: [10.1016/j.jenvman.2010.11.011](https://doi.org/10.1016/j.jenvman.2010.11.011)
10. Ponnusamy, S.K. *Inter. J. Indus. Chem.* **2013**, *4*, 17.
DOI: [10.1186/2228-5547-4-17](https://doi.org/10.1186/2228-5547-4-17)
11. Chen, X.; Mao, S. S. *Chem. Rev.* **2007**, *107*, 2891.
DOI: [10.1021/cr0500535](https://doi.org/10.1021/cr0500535)
12. Huang, D.; Wang, Y.J.; Cui, Y.C.; Luo, G.S. *Micropor. Mesopor. Mater.* **2008**, *116*, 378.
DOI: [10.1016/j.micromeso.2008.04.031](https://doi.org/10.1016/j.micromeso.2008.04.031)
13. Wang, X.; Cao, L.; Chen, D.; Rachel A. Caruso, R.A. *ACS Appl. Mater. Interf.* **2013**, *5*, 9421.
DOI: [10.1021/am401867s](https://doi.org/10.1021/am401867s)
14. Kubacka, A.; Fernandez-Garcia, M.; Colon, G. *Chem. Rev.* **2012**, *112*, 1555.
DOI: [10.1021/cr100454n](https://doi.org/10.1021/cr100454n)
15. Zhang, H.; Hardy, G.C.; Khimyak, Y.Z.; Rosseinsky, M.J.; Cooper, A.I. *Chem. Mater.* **2004**, *16*, 4245.
DOI: [10.1021/cm0492944](https://doi.org/10.1021/cm0492944)
16. Jan, Y-H.; Lin, L-Y.; Karthik, M.; Bai, H. *J. Air & Waste Managem. Assoc.* **2009**, *59*, 1186.
DOI: [10.3155/1047-3289.59.10.1186](https://doi.org/10.3155/1047-3289.59.10.1186)
17. Zhijian, L.I.; Deng, S.; Zhang, X.; Zho, W.; Huang, J.; Yu, G. *Front. Environ. Sci. Eng. China.* **2010**, *4*, 414.
DOI: [10.1007/s11783-010-0241-y](https://doi.org/10.1007/s11783-010-0241-y)
18. Ahmed, M.; Youssef, A.M.; Malhat, F.M. *Macromol. Symp.* **2014**, *96*.
DOI: [10.1002/masy.201450311](https://doi.org/10.1002/masy.201450311)
19. Cao, C-Y.; Cui, Z-M.; Chen, C-Q.; Song, W-G.; Ceria W.C. *J. Phys. Chem. C*, **2010**, *114*, 9865.
DOI: [10.1021/jp101553x](https://doi.org/10.1021/jp101553x)
20. Zhuang, Y.; Yang, Y.; Xiang, G.; Wang X. *J. Phys. Chem. C*, **2009**, *113*, 10441.
DOI: [10.1021/jp9014756](https://doi.org/10.1021/jp9014756)
21. Najafi, M.; Y. Yousefi, Y.; Rafati, A.A. *Sep. Purif. Technol.* **2012**, *85*, 193.
DOI: [10.1016/j.seppur.2011.10.011](https://doi.org/10.1016/j.seppur.2011.10.011)
22. Singh, V.; Preeti, Singh, A.; Singh, D.; Singh, J.; Pandey, A. *Intern. J. Biol. Macromol.*, **2015**, *72*, 261.
DOI: [10.1016/j.ijbiomac.2014.08.016](https://doi.org/10.1016/j.ijbiomac.2014.08.016)
23. Nasiruddin, K. M.; Sarwar, A. *Surface Rev. Lett.* **2007**, *14*, 461.
DOI: [10.1016/j.jhazmat.2006.04.036](https://doi.org/10.1016/j.jhazmat.2006.04.036)
24. Singh V.; Singh, S. K. *Intern. J. Biol. Macromol.* **2011**, *48*, 445.
DOI: [10.1016/j.ijbiomac.2011.01.001](https://doi.org/10.1016/j.ijbiomac.2011.01.001)
25. Singh V.; Kumar, P. *Sep. Sci. & Technol.* **2011**, *46*, 825.
DOI: [10.1080/01496395.2010.534120](https://doi.org/10.1080/01496395.2010.534120)
26. Kumar, K.V. *J. Hazard. Mater.* **2006**, *B137*, 1538.
DOI: [10.1016/j.jhazmat.2006.04.036](https://doi.org/10.1016/j.jhazmat.2006.04.036)
27. McKay, G.; Allen, S.J. *Can. J. Chem. Eng.* **1980**, *58*, 521.
DOI: [10.1002/cjce.5450580416](https://doi.org/10.1002/cjce.5450580416)
28. Singh V.; Tiwari S.; Sharma A.K.; Sanghi, R. *J. Colloid & Interf. Sci.* **2007**, *316*, 224.
DOI: [10.1016/j.jcis.2007.07.061](https://doi.org/10.1016/j.jcis.2007.07.061)

Advanced Materials LettersCopyright © VBRI Press AB, Sweden
www.vbripress.com

Publish your article in this journal

Advanced Materials Letters is an official international journal of International Association of Advanced Materials (IAAM, www.iaamonline.org) published by VBRI Press AB, Sweden monthly. The journal is intended to provide top-quality peer-review articles in the fascinating field of materials science and technology particularly in the area of structure, synthesis and processing, characterisation, advanced-state properties, and application of materials. All published articles are indexed in various databases and are available download for free. The manuscript management system is completely electronic and has fast and fair peer-review process. The journal includes review article, research article, notes, letter to editor and short communications.

